Int. J. Multiphase Flow Vol. 19, No. 4, pp. 575–588, 1993
Printed in Great Britain.

0301-9322/93 $6.00 + 0.00

INTERMITTENT FLOW DRYOUT LIMIT IN HEATED HORIZONTAL TUBES

K. E. CROWE and P. GRIFFITH
Department of Mechanical Engineering, Massachusetts Institute of Technology, Cambridge, MA 02139, U.S.A.

(Received 28 August 1992; in revised form 7 February 1993)

Abstract—The dryout limits for intermittent two-phase flow have been experimentally determined in a horizontal 57 mm conduit operating at atmospheric pressure for a range of heat fluxes in the industrially important range up to 146 kW/m^2. The components of a refined model which incorporates post-slug film drainage, evaporation and measured slugging frequency are introduced. The effect of bubble nucleation in the post-slug film was observed and appears to be unimportant. The model is generally conservative in its prediction of the dryout boundary and shows a heat flux dependence not reflected in the data.

Key Words: dryout, flow regimes, nucleation, slug flow, slug frequency, stratified flow

INTRODUCTION

The allowable operational range of horizontal boiler tubes is determined, among other things, by pumping power and pipe life. A serious threat to pipe operating life is film dryout on the upper tube wall, leading to unacceptably high temperatures or thermal cycling of the tube material. Typically, this can be avoided if the mass flux is sufficiently high, but higher pumping power costs are then incurred. In addition, knowledge of the wall boundary condition and phase distribution is important in predicting two-phase heat transfer and pressure drop, so it is necessary to know the conditions under which the wall is dry.

Three types of dryout exist in horizontal flow. The low-quality or stratified dryout is well-understood. High-quality or annular-flow dryout is inevitable as the pipe begins to run out of liquid (Biasi *et al.* 1967). Moderate quality or intermittent dryout is not well-understood, but is believed to be limiting with respect to the acceptable mass flux levels (Bar-Cohen *et al.* 1987). Slug flow or intermittent dryout is accompanied by oscillations in pipe temperature which may, in fact, be more damaging than high absolute temperatures.

Intermittent dryout has been identified in the high-pressure studies of Lis & Strickland (1970) and Styrikovich & Miropolski (1956). Fisher & Yu (1975) have studied intermittent dryout using higher pressure R-12. Most recently, Ruder *et al.* (1986, 1987) and Bar-Cohen *et al.* (1986, 1987) found intermittent dryout boundaries for atmospheric steam–water in a 25.4 mm horizontal tube at relatively low heat flux and successfully mapped them using superficial velocity coordinates commonly used to show flow regime boundaries. Ruder's simple model to predict intermittent dryout is slightly conservative in its prediction of critical liquid velocity but predicts that, for higher heat flux, the intermittent dryout region will exist at higher liquid superficial velocities than the stratified flow limit.

The purpose of this project was to determine the dryout limits for two-phase flow in horizontal conduits using industrially relevant conditions with emphasis on the effects of pipe size and heat flux. The experimental work focused on 57 mm pipes for heat fluxes up to 146 kW/m^2. The system was designed to run at atmospheric pressure to allow for simplicity in fabrication and greater flexibility. Ruder's (Bar-Cohen *et al.* 1986) model has been modified and compared to the data. The intent for the model is to extrapolate to higher pressure where little dryout data currently exists (Lis & Strickland 1970; Styrikovich & Miropolski 1956).

EXPERIMENTAL APPARATUS

With these considerations, the horizontal flow test rig was designed and fabricated. It is shown schematically in figure 1. The closed flow loop begins in the holding tank, which acts as a reservoir and steam–water separator. The slightly subcooled liquid is pumped with an 18.2 m^3/h, 138 kPa impeller pump, controlled with main and by-pass globe valves and measured with a 31.8 mm turbine meter, manufactured by Hoffer Flow Controls, which has a linear range between 1.36 and 21.1 m^3/h. The flow enters the single tube-in-shell condensing preheater to reach a two-phase state before entering the test section. High-quality 414 kPa steam feeds the separator which provides saturated steam to the preheater.

The thin-walled (schedule 5) stainless-steel test section has an overall length of 2 m. Stainless steel was chosen for its high electrical resistance, its ability to withstand extreme temperatures and repeated dryouts and its corrosion resistance. The wall thickness was chosen to produce the optimal electrical resistance to achieve maximum power dissipation from the 45 kW, 3000 A, DC power supply. A secondary benefit is the rapid thermal response of the 1.65 mm thick wall. As a result, much of the temperature history information is not filtered out by the pipe capacitance so the temperature measurements can be used for statistical analysis of the data.

A sight glass at the outlet allows for visual observation of the flow regime. The goose neck prevents a stratified flow at the discharge from affecting the upstream void fraction. It simulates the rising serpentine tubes often found in fluidized bed combustors, economizers and waste heat heat exchangers. A large-diameter (102 mm) pipe was used thereafter to minimize the two-phase pressure drop. Within the holding tank, there are four 7.6-m lengths of 9.5 mm copper tube using tap water to condense the produced steam.

With the exception of the test section, copper pipe is used throughout to minimize the corrosion. Type K thermocouples were inserted as shown to measure the inlet subcooling and to calibrate the preheater. None of the system was insulated, except for small regions over each test-section thermocouple. The overall heat loss was calculated not to exceed about 6% and could be reliably accounted for. The benefit of achieving a rapid and reliable steady state upon changing thermal or hydrodynamic conditions outweighed the loss of accuracy in the energy balance.

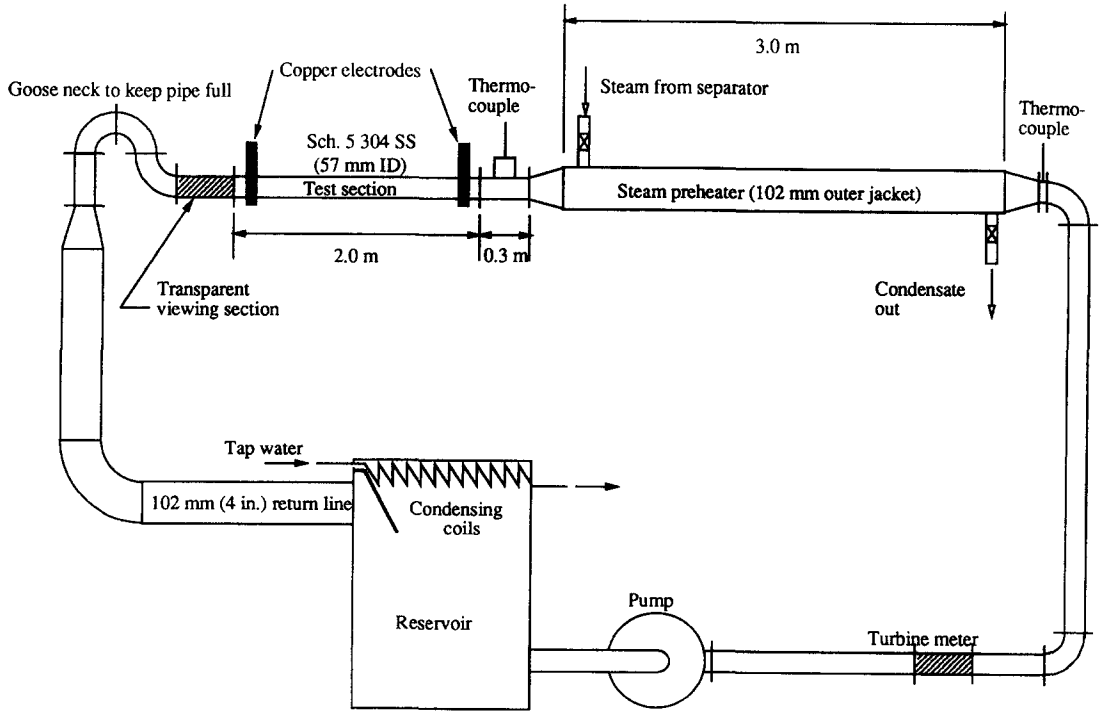

Figure 1. Sketch of the atmospheric pressure rig with a 57 mm test section.

For the determination of the dryout state, the test section was instrumented with 10 differential thermocouple sets spaced at uniform 203 mm intervals along the length. An example of a thermocouple set assembly is shown schematically in figure 2. The unsheathed type K thermocouples were welded and placed against the pipe with a thermally conducting, electrically insulating layer between them. Omega Thermcoat CC cement was essential to isolate the thermocouple from the electric potential present in the metal pipe. To insure thermal equilibrium with the pipe, a 50 mm square of 25 mm thick quartz wool covered each thermocouple and the whole assembly was held on with two 5-cm square curved aluminum sheets and a hose clamp. The thermocoupled sets were wired differentially at terminal connectors located near the pipe. Extension grade thermocouple wire brought the signal to the Metrabyte EXP-16 multiplexer board. This board employed a gain of 1000 and was connected to the IBM AT computer's DASH-16F board. Labtech Notebook version 4.3 was used for the data acquisition. With 10 differential inputs, the computer could sample each at 15 Hz, which was sufficient to resolve the system thermal frequency.

EXPERIMENTAL METHODOLOGY

The determination of dryout using external temperature information is somewhat arbitrary. Ruder (1984) used the difference in the steady-state-averaged temperature between top and bottom as the criterion. Since the bottom is always wet in horizontal flow, it was assumed that a positive difference of $\Delta T = T_t - T_b$ exceeding some threshold indicates dryout. At least two difficulties arise using this approach. First, the imprecision inherent to thermocouples does not allow for use of a small dryout temperature threshold. To deal with this, one would have to accept a large threshold to reliably conclude anything about the thermal state. The dryout bounds may as a result be severely underestimated or missed completely. Secondly, one cannot assume that a positive ΔT, no matter how small, is an indication of *impending* dryout. If no dryout is present in slug flow, the time-averaged heat transfer coefficient, h, at the tube top has contributions from a boiling/convection h as the slug passes, weighted with a film evaporation h as the bubble passes. Along the bottom, only the boiling/convection h applies. Since the heat transfer coefficient, h, for an evaporating film is substantially higher, the average h, under pre-dryout conditions, is higher—leading to a lower average wall temperature under uniform flux conditions. So, with dryout impending in the slug flow regime, it can be shown that ΔT is actually negative. Instances where $\Delta T < 0$ are found in the data of Ruder (Ruder *et al.* 1987; Bar-Cohen *et al.* 1987). Use of a positive ΔT threshold to show the incipience of slug flow dryout is likely to either misinterpret the flow regime, or indicate only those dryout conditions that are extreme enough.

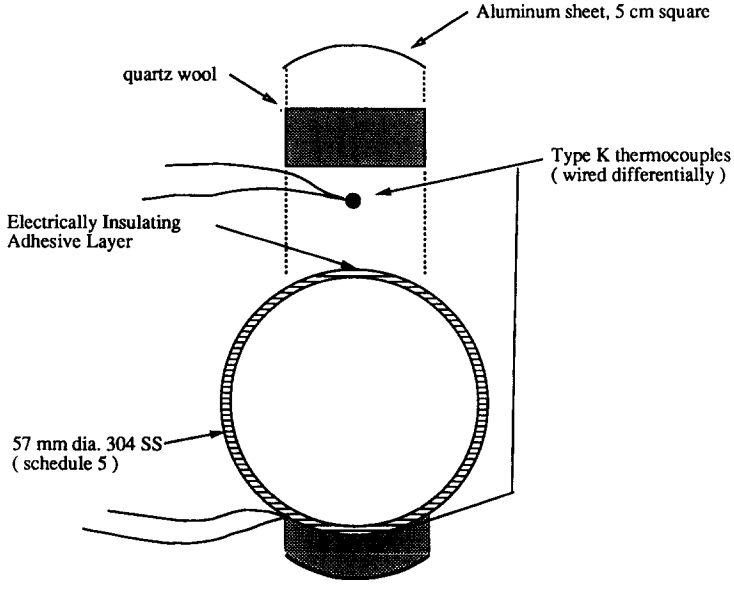

Figure 2. Sketch of the differential thermocouple assembly.

A solution to these dilemmas is proposed here. If one preserves all of the temperature history information, i.e. $\Delta T(t)$, and analyzes this data without regard for a baseline temperature, the thermocouple errors noted above are reduced substantially. In effect, the absolute ΔT is ignored and the assessment is made from the fluctuations of ΔT. Clearly, the set-to-set variations due to thermocouple imprecision and multiplexer channel imprecision are cancelled out and the only uncertainty arises from differing thermocouple response constants, which are certainly within a few percent.

An advantage to this approach is that the temperature history is saved, allowing for statistical analysis in any number of ways. More fundamentally, the actual problem associated with slug flow dryout can be seen: the fluctuation of pipe temperature with time.

When the system achieved steady state, the liquid rate and inlet quality were varied to cover the entire slug flow region of the flow regime map. Heat flux was a parameter. For each run, data was taken on all channels for 2 min. The $\Delta T(t)$ data was smoothed to minimize the effect of noise using a 5-point nearest temporal neighbor averaging technique, which gave effective smoothing while not "filtering" the signal drastically. A typical portion of a differential temperature trace is shown in figure 3, which includes the derived quantities used throughout.

INTERMITTENT DRYOUT RESULTS

Using the previously described experimental procedure, thermal bounding maps were constructed at four different heat fluxes up to 146 kW/m^2 (corresponding to the maximum available power). The results are shown in figures 4–7. Each velocity–quality pair (or $j_L j_G$) is mapped with the corresponding thermal state. Lines of constant quality are shown for reference. Typically, the data points appear in groups of 10—corresponding to the 10 thermocouple locations. Since the map is on log–log coordinates, the points lie closer together for increasing quality. Sometimes points overlap where the mass flow and quality are identical but a differing inlet quality is employed.

In general, four states have been distinguished. The + signs represent points where dryout does not occur. The ■ symbols are where it is believed dryout resulting from flow stratification occurs.

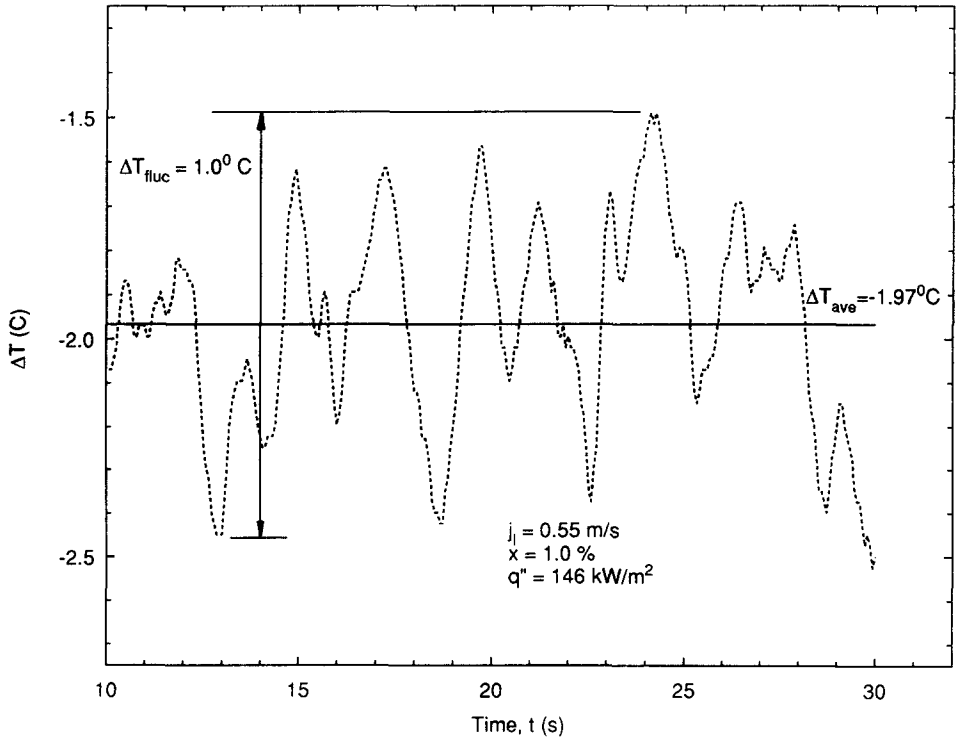

Figure 3. A 20 s portion of a smoothed differential temperature trace showing the defined nomenclature.

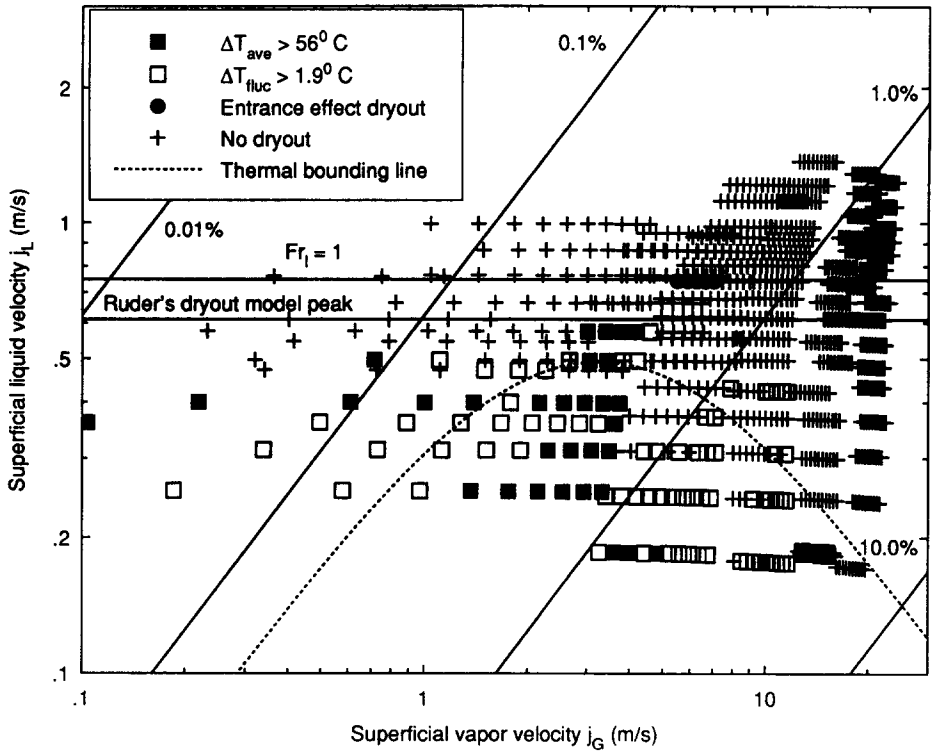

Figure 4. Dryout map for $q'' = 37\ \text{kW/m}^2$.

The criterion for these points is that the time-averaged temperature difference from top to bottom (ΔT_{ave}) exceeds 56°C (100°F). Although somewhat arbitrary, it is clear that to sustain a temperature difference of this magnitude, the rewetting of the tube must be so infrequent that the flow is effectively stratified. The data falling under this ΔT_{ave} criterion was not strongly affected by

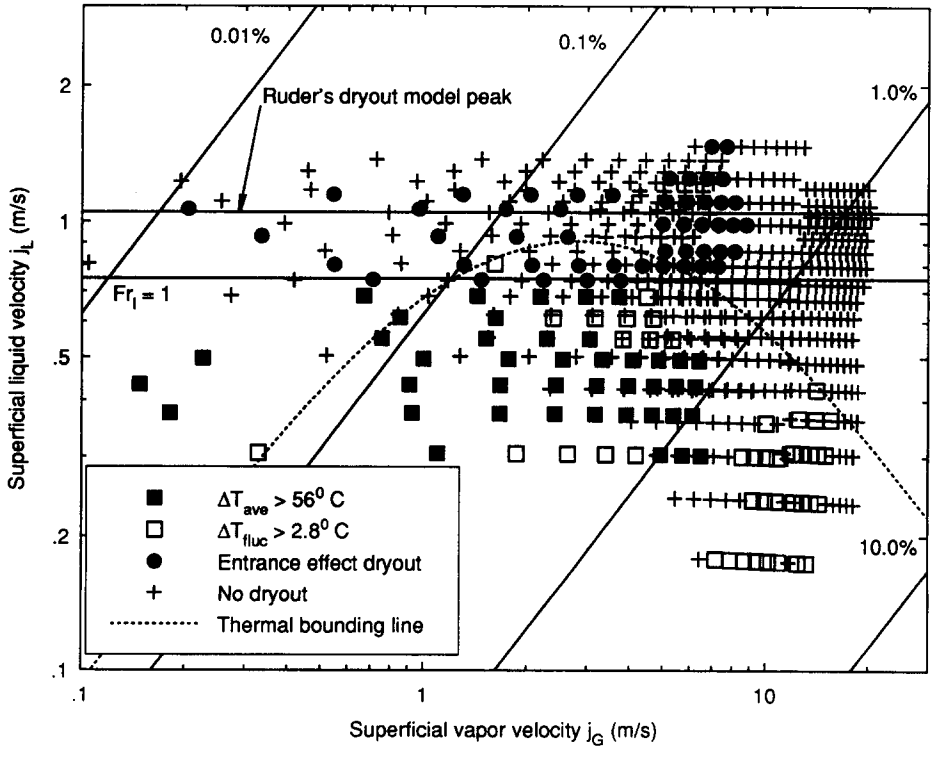

Figure 5. Dryout map for $q'' = 71\ \text{kW/m}^2$.

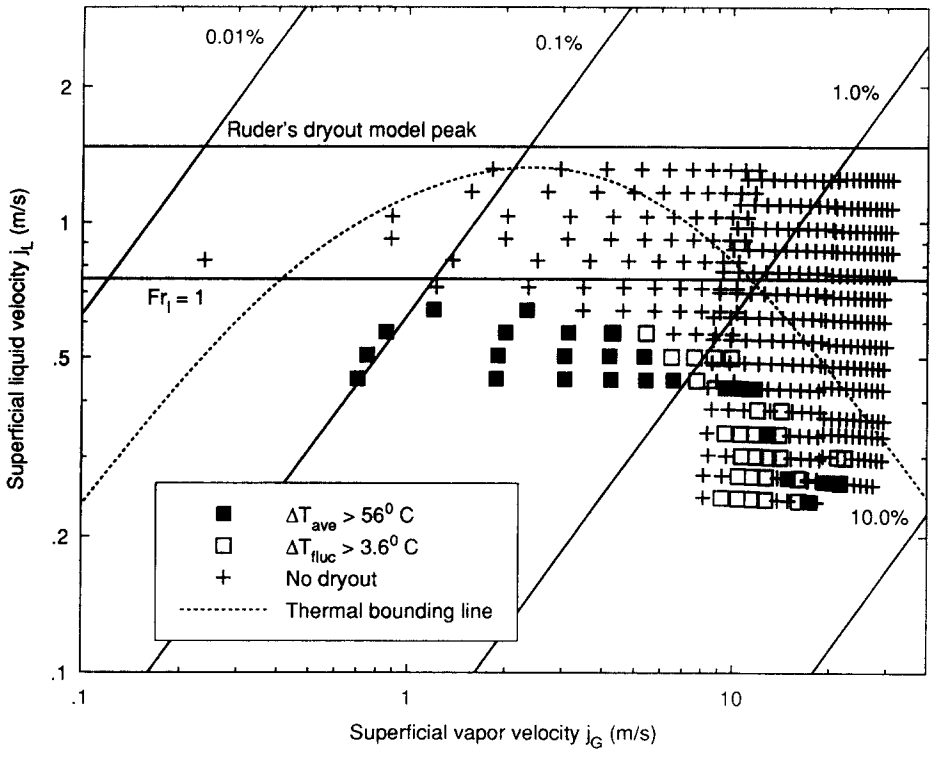

Figure 6. Dryout map for $q'' = 106\ \text{kW/m}^2$.

change in this threshold value. No information from temperature fluctuations is used for these points.

The □ are points where it is believed *intermittent* dryout is occurring. Though ΔT_{ave} is small or often negative, the magnitude of the total fluctuation in ΔT exceeds the chosen threshold, which

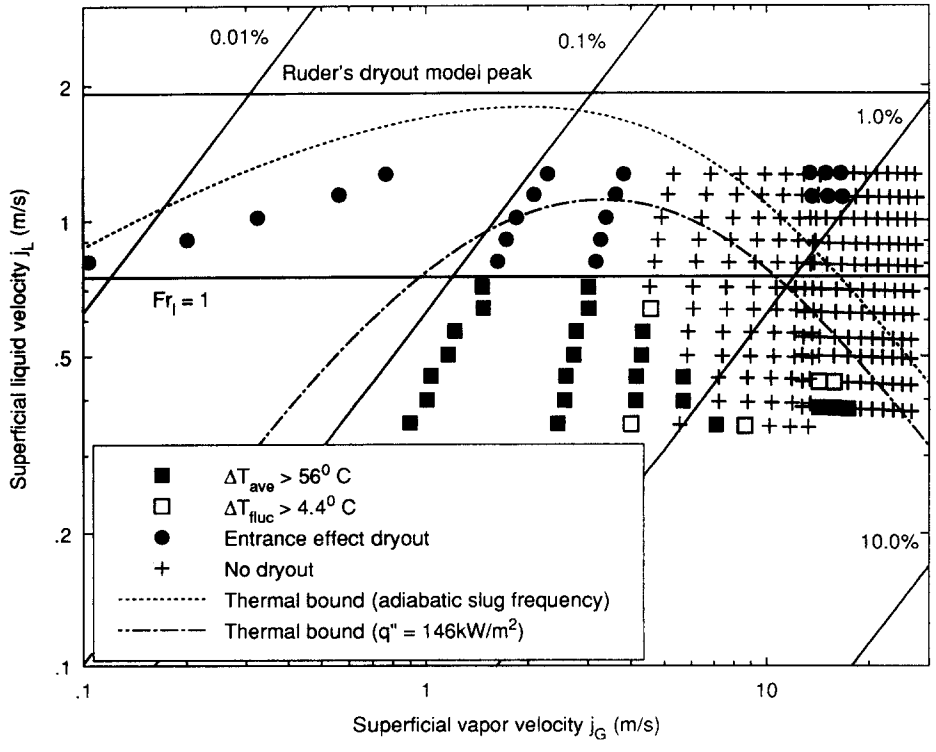

Figure 7. Dryout map for $q'' = 146\ \text{kW/m}^2$.

is given on each map. Clearly, periodicity of the flow produces a varying heat transfer coefficient at the tube top, and one would expect temperature fluctuations in all cases of intermittent flow. However, the presence of a transient dry wall would be expected to increase the amplitude of this fluctuation. Thus, the onset of intermittent flow dryout is inferred when ΔT_{fluc} exceed the defined threshold value. The transient response of the pipe wall was analyzed and the temperature amplitude depends on the heat flux and slug period, but is of order 2–5°C. The electrically insulating layer and thermocouple, which have a time constant of the same magnitude as the pipe itself, will tend to damp the response further, reducing this temperature amplitude. Therefore, the threshold was chosen to be a minimum value that left a contiguous region of map points. Using smaller values incorporated additional *isolated* points not associated with a true dryout. In addition, the threshold value was scaled linearly with heat flux. It should be noted that the criterion for ΔT_{ave} took precedence over that for ΔT_{fluc}, since a large ΔT_{ave} may have associated unsteadiness, yet be indicative of continuously dry wall.

The state shown by the ● symbols indicates dryout resulting from a local adverse condition existing at the test section inlet. These dryouts are characterized by a large ΔT_{ave} ($\Delta T_{ave} > 56$°C), but occur at mass velocities that are too large to be explained by a simple Froude number (Fr) argument for stratified flow. This will be discussed in more detail later.

DISCUSSION OF RESULTS

Referring to figure 4, it is seen that the stratified or high ΔT dryout occurs for qualities, x, less than about 1% and for liquid superficial velocities, j_L, less than about 0.7 m/s. This finding is consistent with the hydrodynamic boundaries for stratified flow (Dukler & Taitel 1986). Though the fluctuation in ΔT is substantial, the large ΔT is indicative of an essentially dry wall.

For x between about 1 and 3% and below j_L of about 0.5 m/s exists the intermittent dryout region (also referred to as the *dome*). It should be noted that there is a region between the stratified and intermittent dryout regions where the tube is wet. Because ΔT_{ave} is smaller, the flow is no longer stratified but the slug flow apparently has not developed to the point where dryout results. That is, the bubbles are not yet so long that dryout occurs between slugs. Also, the termination of the dome on the right side does not imply the termination of slug flow. The flow was verified at the test section exit to be intermittent in these runs, so the termination of the intermittent dryout precedes the termination of slug flow. Clearly, the intermittent dryout region is a subset of the slug flow region.

The peak of this dome is of chief concern and lies at about 0.45 m/s. For this relatively low heat flux, this peak, or the minimum superficial liquid velocity ($j_{L_{min}}$) to avoid dryout is less than the limit given by low quality of stratified dryout. This means the stratified limit governs. The remaining maps (figures 5–7) indicate the same basic structure. The two defined dryout regions appear in approximately the same locations. The stratified limit varies somewhat but is always less than $Fr_L = 1$. The peak of the intermittent dome is always less than the low quality dryout limit ($Fr_L = 1$) and is nearly constant at about 0.45 m/s. Based on the extrapolation of Ruder's model, the slug flow peak, was expected to be the limiting dryout boundary for the 57 mm pipe at these heat fluxes. This striking result indicates that although Ruder's model was reasonable for lower heat fluxes, it is much too conservative at high heat flux and requires some refinement. This also means slug flow dryout takes on diminished importance.

The dryout points toward the upper part of the map which have an associated high ΔT could not at first be explained, because the mass flux is far too large to support a stable stratified flow. It was observed that the physical location of all these points was near the pipe inlet extending in some cases down the entire pipe length. It was noted that there was a 6 mm step increase in diameter at the junction of the preheater and the test section (see figure 1) and perhaps this was a sufficient disturbance to cause stratification. To visualize the problem, a transparent section having the same inside diameter as the test section was inserted between the preheater and the test section. When the system was run at high single-phase velocities near the saturation temperature, it was found that the flow stratified such that a long vapor pocket trailed off the junction and into the test section. Figure 8 shows a photograph of such a pocket. The flow, with $Fr_L > 1$, is from left to right. The appearance of condensate on the upper half of the lexan tube indicates that an extended time

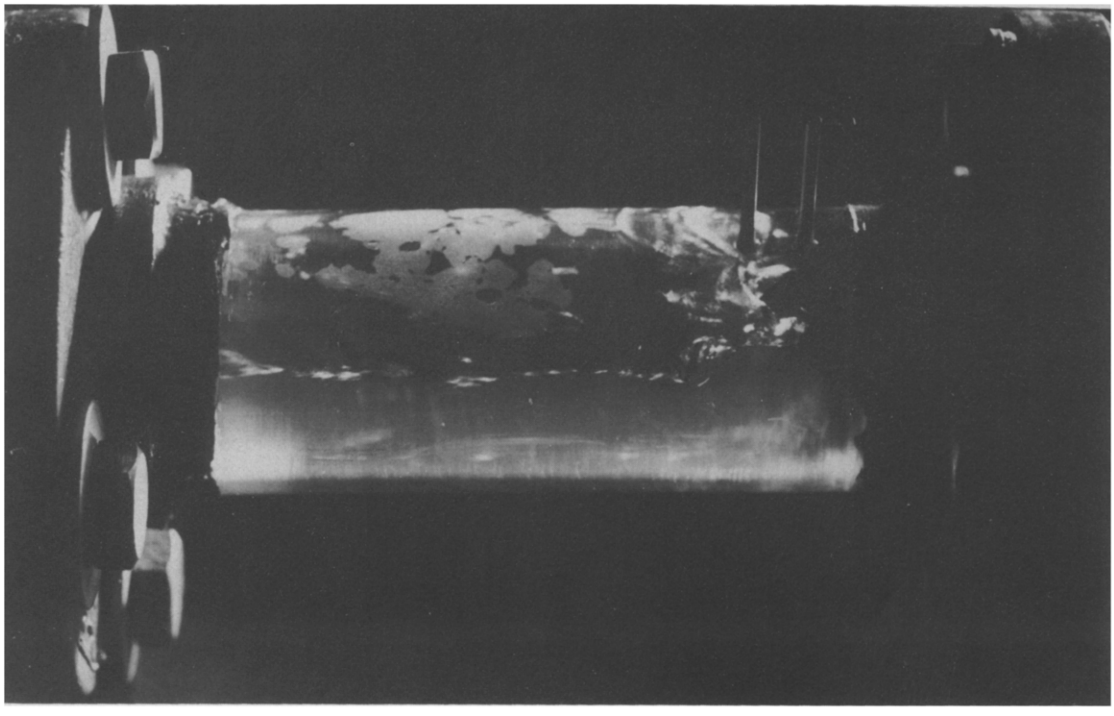

Figure 8. Photograph of a stationary vapor pocket viewing downward at 45°.

period has elapsed since the surface was wetted. The vapor pocket was relatively stable, but could not be systematically reproduced. This is consistent with the fact that not all the maps show this type of state. The observation of this vapor pocket confirms the cause of the unexpected dryout. Also it confirms the conclusions of Lis & Strickland (1970), that inlet effects can lead to pipe anisothermality. In those experiments, overheating occurred downstream of hairpin bends. In the present work however, what would be considered a minor disturbance (small diameter change) led to a serious problem. An important conclusion to draw is that the fabrication details of a piping system can have a marked impact on the local thermal behavior. These observations strongly reinforce those of Lis & Strickland (1970).

MODELING OF INTERMITTENT DRYOUT

First attempts at physically based dryout models have been made principally by Ruder (Bar-Cohen *et al.* 1986) and by Coney (1974). Essentially, slug flow is treated as a periodic phenomenon and the characteristic period is balanced with the time to dryout based on the combined effects of the different mechanisms. Ruder considers two effects tending to remove liquid from the wall, namely the post-slug liquid film drainage down the tube wall and evaporation of this film driven by the imposed heat flux. These effects are considered as acting separately, but are in fact dependent. The total contribution due to drainage was shown to be small compared to evaporation and was neglected. However, a parameter needed in the analysis, the initial value of the film thickness was assumed to be 50 μm and appears to be quite dubious. It will be shown that the initial film thickness is substantially larger but in fact does not strongly influence the problem for the values calculated. Ruder then balances the time to evaporate the film with an empirically determined slug frequency correlation for fully-developed adiabatic slug flow.

The work of Coney (1974) is certainly more detailed but was not presented within the context of dryout data. A detailed fluid mechanical analysis is given where emphasis is placed on the initial after-slug film thickness and the inertial effects in the falling film. Simulation results are compared favorably with adiabatic drainage data.

A model is presented incorporating drainage, evaporation and measured slug frequencies for both adiabatic and diabatic flow in a pipe of typical (though not necessarily fully developed) length. The effects of bubble nucleation within the film are discussed.

DRAINAGE AND EVAPORATION

The sketch in figure 9 shows a pipe cross section with a film of thickness δ_0 on the upper half of the wall and a thick liquid layer in the bottom. This corresponds to a time after a slug has passed. The details of this model can be found in Crowe (1992), the results of which are presented here. If one considers only the tube top, an evolution equation can be obtained with the combined effect of evaporation and drainage. This has also been shown in the work of Gardner (1972). The governing equation is

$$\frac{d\delta}{dt} = \frac{-q''}{\rho_L h_{LG}} - \frac{g\delta^3}{3\nu R}, \qquad [1]$$

subject to the initial condition; in [1] δ is the liquid film thickness, q'' is the heat flux, ρ is the density, h_{LG} is the evaporation enthalpy, ν is the kinematic viscosity and R is the pipe radius, the subscripts L and G refer to liquid and gas, respectively.

The appropriate initial thickness, δ_0, corresponds to the onset of viscously dominated flow, since the governing equation is based on this limit. Inertially dominated flow occurs for the free-fall duration, t_{ff}:

$$t_{ff} \approx \sqrt{\frac{2R}{g}}, \qquad [2]$$

which for a 25 mm radius tube is on the order of 0.1 s; g is the gravitational acceleration. Only liquid that is within the developing boundary layer is not subject to free fall. The thickness of this boundary layer is approximately given by

$$\delta_{bl} \approx 4\sqrt{\nu t} \qquad [3]$$

or about 1.0 mm. This thickness will be taken to be δ_0.

The solution $t(\delta)$ is

$$t = \frac{-\epsilon}{3a}\left[\frac{1}{2}\ln\left[\frac{(\delta+\epsilon)^2}{\delta^2 - \epsilon\delta + \epsilon^2}\right] + 3\arctan\left(\frac{2\delta - \epsilon}{\epsilon\sqrt{3}}\right)\right]_{\delta_0}^{\delta=0}, \qquad [4]$$

where the void fraction

$$\epsilon = \left(\frac{3q''\nu R}{\rho g h_{LG}}\right)^{1/3} \text{ and } a = \frac{q''}{\rho_L h_{LG}}.$$

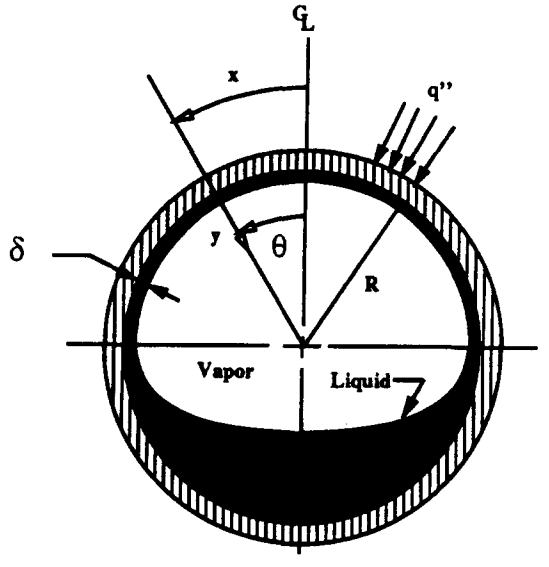

Figure 9. Sketch of the pipe cross section with a draining film.

To obtain δ explicitly as a function of time, it was necessary to invert the coordinates numerically. Figure 10 shows the simulated thickness evolution for the four heat fluxes used. The times to dry out the film are given along the axis. Use of this result will be discussed subsequently.

Bubble nucleation

At the relatively high heat fluxes in question here, it is not known whether all phase change takes place at the film surface, i.e. evaporation, or whether some takes the form of bubbles growing at the heated wall. In the latter case, the effects on film depletion are not known. Several effects may include: (a) liquid loss due to droplet entrainment into the vapor when bubbles burst; (b) de-wetting due to surface tension if the bubble bursts and forms a true discontinuity in the film; (c) impedance to the drainage process since the bubbles may be considered as obstacles; and (d) displacement of the surrounding film as bubble growth proceeds, thereby increasing the local film thickness, *augmenting* drainage.

To study the effect of nucleation in the film, a small test rig was built. The details of this experiment are given in Crowe (1992). A major conclusion from this study was that nucleation is suppressed very shortly after initiation of film drainage due to the rapid thinning. Dryout of the film usually occurred in a few small locations after a short time; a time which depended on the heat flux. This was followed by a rapid dryout of the complete upper half of the tube shortly thereafter, indicating that as the film thins, it becomes very uniform. It may be expected then, that if dryout occurs, large dry patches result.

Although the existence of nucleate boiling in the film was confirmed for a range of heat fluxes, it appears that its effect on dryout is benign. The boiling sites only covered a small part of the pipe area, did not lead to rupturing the film, and did not produce a large mass of entrained droplets. In addition, the nucleate boiling was suppressed rapidly during film drainage eliminating its effect.

SLUG FREQUENCY

The mechanisms depleting the wall of the liquid film are connected to dryout by the frequency of slugging, which depends most strongly on the superficial velocities of the two-phase mixture.

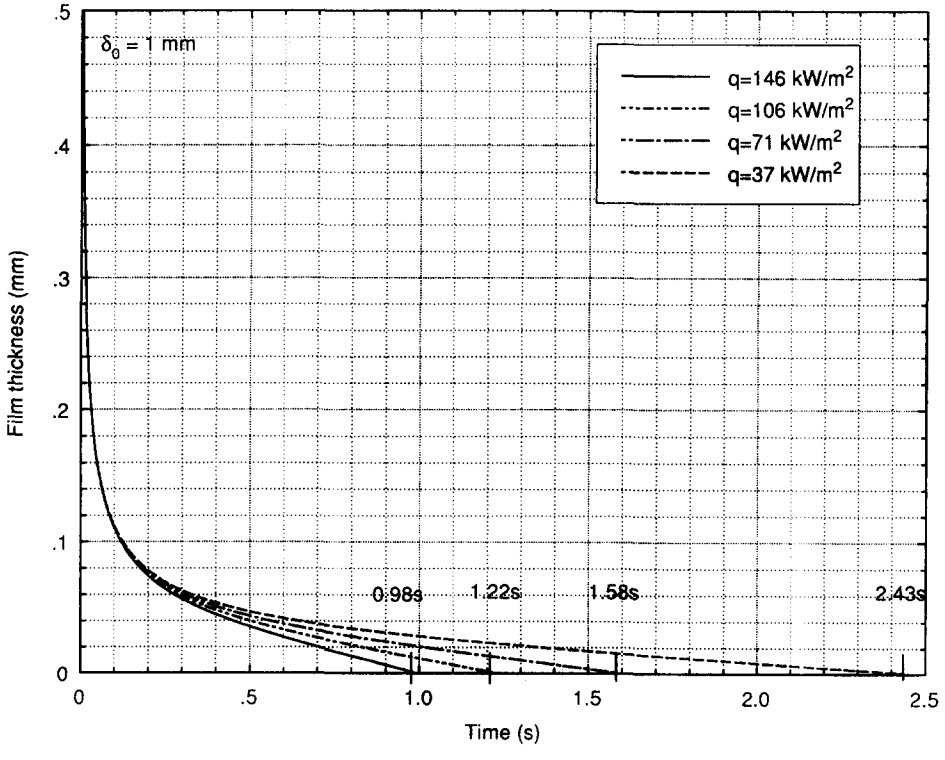

Figure 10. Calculated film thickness evolution, [4], for four heat fluxes.

Prescribing the necessary frequency gives the necessary minimum liquid velocity $j_{L_{min}}$. Slug frequency has been experimentally studied by Gregory & Scott (1969) and Greskovich & Shrier (1972). The flows considered were fully developed ($L/D \geqslant 300$) and typically for sizes of pipe < 51 mm. Their correlation was used by Ruder to construct the previous dryout model (Ruder, 1984) but three issues arise which lead one to question its applicability in the present study. These concern pipe diameter range, the application of heat flux and the existence of developing flow.

Experimental determination of slug frequency

To check the applicability of the fully-developed, adiabatic slug frequency correlation, the slug frequency was measured for the range of superficial velocities encountered in the diabatic experiments. Slug detection was performed using a variation of the flush conductance probe described by Hewitt *et al.* (1964). For given flow conditions, the number of slugs was counted from the probe's voltage–time trace which was sampled at 20 Hz for 4 min. Measurements were made for both adiabatic and heated conditions using $q'' = 146\ \text{kW/m}^2$. The resulting frequencies were compared with the Gregory & Scott (1969) correlation.

The slug frequency was plotted against the same form of the function used in that study with the constants adjusted. This approach is justified because the previous correlation was formed on three observations of the data which are believed to apply here as well: (a) the slug frequency increases directly with j_L and inversely with D (the pipe diameter) (b) a frequency minimum exists with respect to the slug velocity which is (c) proportional to the "no-slip velocity", $j_L + j_G$. The function is given by

$$v_s = a\left\{\frac{j_L}{gD}\left[(j_L + j_G) + \frac{b}{j_L + j_G}\right]\right\}^c \qquad [5]$$

where for the Gregory & Scott experiments $a = 0.0226$, $b = 44.75$ and $c = 1.2$. In this work, the values of a, b and c were optimized to give a least-squares fit to the present data. The plots in figures 11 and 12 show the frequency vs the above correlation function for the unheated and heated cases, respectively. As seen in both plots, there is some scatter but the data gather around the unit slope straight line which nearly intersects the origin as expected.

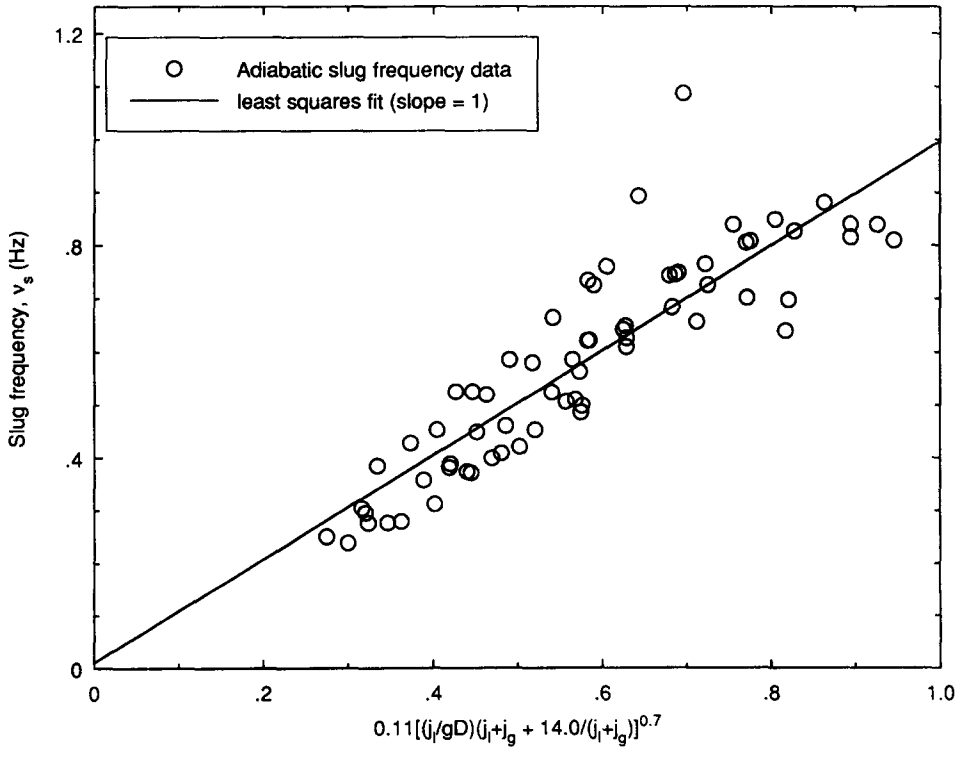

Figure 11. Adiabatic slug frequency vs correlation function.

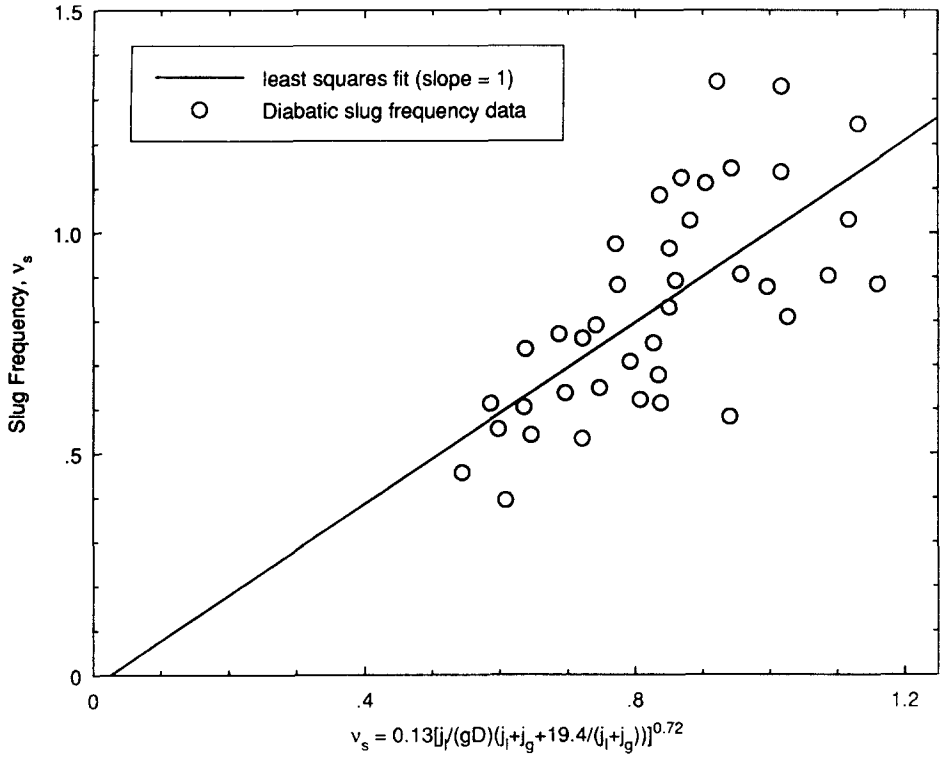

Figure 12. Diabatic (146 kW/m^2) slug frequency vs correlation function.

The measured frequencies for the unheated case are substantially larger than those calculated using the Gregory & Scott (1969) correlation and may explain the conservative estimate or Ruder's (1984) model. This may be explained, in part, because the system length is less than that required for full slug development. The bubble length required such that consecutive slugs do not interact has not been attained. Slugs shorter than the turbulence dissipation length would tend to coalesce, making longer slugs and bubbles, thereby decreasing the frequency. Since the system length in this problem is typical of industrial stream generators, it is appropriate to use a measured frequency for this system for comparison to the thermal data and for construction of a dryout model.

The slug frequency for diabatic flow was measured for one heat flux to show the effect qualitatively. The quantitative dependence is not known but the frequencies found in the heated cases are larger. This confirms the speculation of Ruder *et al.* (1987) as to why the dryout dome peak is seemingly independent of heat flux. The increase is probably the result of increased void in the liquid portion of the flow. This additional vapor in the liquid increases the effective *liquid* superficial velocity, which will affect a higher slug frequency. The bubbly flow configuration has a limit of about $\epsilon = 25\%$, which to first order, will raise the effective liquid superficial velocity by about one-third (Dukler & Taitel 1986). This is consistent with the augmentation seen in the heated frequency data.

SEMI-ANALYTICAL THERMAL BOUNDARY

With the components of this model discussed, assembling of the thermal boundary requires use of [4] and [5]. The time to dry out the film was calculated for each heat flux and is shown in figure 10. The slugging frequency correlation was solved iteratively for j_L for a range of j_G. The result is the semi-analytic thermal bound (dome) given on each of the maps (figures 4–7).

The dome-like appearance is related to the fact that there exists a minimum in the slug frequency with respect to the sum $j_L + j_G$. The agreement between this bound and the intermittent dryout data (□) clearly depends on the heat flux. Reasonable agreement in the critical liquid velocity, $j_{L_{min}}$ occurs at $q'' = 37$ kW/m^2 but increasing heat flux gives rise to an increasingly conservative result. For the highest heat flux, the thermal bound is shown using the present *diabatic* slug frequency

correlation. As seen, using the augmented frequency has substantially lowered the peak of the predicted dryout zone; however, it is still quite conservative. The rather strong dependence of the analytical result on the heat flux is not surprising; rather, the seeming independence of the data to heat flux is more perplexing. The augmentation of the slug frequency with heat flux has provided a partial explanation for this behavior. The remaining discrepancy may be in the comparison of the calculated dryout of the tube upper surface and the inference of dryout based on external temperature measurements. However, it can be stated that benign temperature oscillations will result if the liquid velocity is maintained above the stratified flow limit.

CONCLUSIONS

- The minimum liquid superficial velocity to avoid dryout, which exists at the peak of the dryout dome in the intermittent regime is appreciably less than that predicted by the Ruder *et al.* (1987) model. The present model, which considers film drainage and measured slug frequency, does a slightly better job but shows a heat flux dependence not reflected in the data.
- The heat flux dependence in the present model is partially countered by a small increase in the slug frequency with heat flux. Hence, heat flux is not an important variable in determining the intermittent dryout limit.
- Bubble nucleation was seen to exist over most of the heat flux range but its effect on film depletion is deemed negligible. This conclusion is expected to be valid at high pressure too because the superficial velocity of evaporating vapor normal to the wall will decrease at high pressure.
- Fabrication details of the piping system can have a significant impact on the local wall temperature. Stratification leading to dryout can occur if an unfavorable disturbance like a small step increase in diameter is encountered at low quality, even though $Fr_L > 1$.
- It was found that the intermittent flow dryout limit is significantly less than the low-quality dryout limit given by $Fr_L \leqslant 1$. Therefore, scaling or large diameters, high pressure and high heat flux in the intermittent regime has diminished importance. The stratified flow limit will govern the minimum acceptable flow velocity in a horizontal tube.

Acknowledgements—We would like to thank the Department of Energy for the funding that made this work possible. Also, for fabrication of the essential hardware of the test rig and continuous technical support, we thank J. A. Caloggero of the Mechanical Engineering Department at MIT.

REFERENCES

BAR-COHEN, A., RUDER, Z. & GRIFFITH, P. 1986 Development and validation of boundaries for circumferential isothermality in horizontal boiler tubes. *Int. J. Multiphase Flow* **12,** 63–77.

BAR-COHEN, A., RUDER, Z. & GRIFFITH, P. 1987 Thermal and hydrodynamic phenomena in a horizontal, uniformly heated steam-generating pipe. *J. Heat Transfer* **109,** 739–745.

BIASI, L., CLERICI, G. C., GARRIBBA, S., SALA, R. & TOZZI, A. 1967 Studies on burnout, Part 3—a new correlation for round ducts and uniform heating and its comparison with world data. *Energ. Nucl.* **14,** 530–536.

CONEY, M. W. E. 1974 The analysis of a mechanism of liquid replenishment and draining in horizontal two-phase flow. *Int. J. Multiphase Flow* **1,** 647–669.

CROWE, K. E. 1992 Flow regimes and dryout in horizontal heated tubes. Ph.D. Thesis, Dept of Mechanical Engineering, MIT, Cambridge, MA.

DUKLER, A. E. & TAITEL, Y. 1986 Flow pattern transition in gas–liquid systems: measurement and modeling. In *Multiphase Science and Technology* (Edited by HEWITT, G. F., DELHAYE, J. M. & ZUBER, N.), pp. 1–94. Hemisphere, Washington, DC.

FISHER, S. A. & YU, S. K. M. 1975 Dryout in serpentine evaporators. *Int. J. Multiphase Flow* **1,** 771–791.

GARDNER, G. C. 1972 Drainage and evaporation of a liquid film with salt depositon upon a horizontal cylindrical surface. *Int. J. Heat Mass Transfer* **15,** 2063–2075.

GREGORY, G. A. & SCOTT, D. S. 1969 Correlation of liquid slug velocity and frequency in horizontal cocurrent gas–liquid slug flow. *AIChE Jl* **15,** 933–935.

GRESKOVICH, E. J. & SHRIER, A. L. 1972 Slug frequency in horizontal gas–liquid slug flow. *Ind. Engng Chem. Process Des. Dev.* **11,** 317–318.

HEWITT, G. F., KING, R. D. & LOVEGROVE, P. C. 1964 Liquid film and pressure drop studies. *Chem. Process Engng* **April,** 191–200.

LIS, J. & STRICKLAND, J. A. 1970 Local variations of heat transfer in a horizontal steam evaporator tube. *Proc. 4th Int. Heat Transfer Conf.* **5,** paper 4.6.

RUDER, Z. 1984 The influence of two-phase flow regimes on circumferential temperature distribution in horizontal, steam generating tubes. Ph.D. Thesis, Dept of Mechanical Engineering, Ben Gurion Univ., Israel.

RUDER, Z., BAR-COHEN, A. & GRIFFITH, P. 1986 An example of the application of the bounding dryout criteria in horizontal steam generating tubes for the case of circumferentially nonuniform heat flux. *Int. J. Multiphase Flow* **12,** 845–852.

RUDER, Z., BAR-COHEN, A. & GRIFFITH, P. 1987 Major parametric effects on isothermality in horizontal steam generating tubes at low- and moderate qualities. *Int. J. Heat Fluid Flow* **8,** 218–227.

STYRIKOVICH, M. A. & MIROPOLSKI, Z. L. 1956 On the effect of tube inclination on circumferential isothermality. Report No. IGRL-T.R4.